Eur. Phys. J. C 47, 263–271 (2006)
Digital Object Identifier (DOI) 10.1140/epjc/s2006-02559-9

THE EUROPEAN PHYSICAL JOURNAL C

Investigating halo substructures with annual modulation signature

R. Bernabei[1,a], P. Belli[1], F. Montecchia[1], F. Nozzoli[1], F. Cappella[2], A. Incicchitti[2], D. Prosperi[2], R. Cerulli[3], C.J. Dai[4], H.L. He[4], H.H. Kuang[4], J.M. Ma[4], X.D. Sheng[4], Z.P. Ye[4,b], M. Martinez[5], G. Giuffrida[6,7]

[1] Dip. di Fisica, Universita' di Roma "Tor Vergata" and INFN, sez. Roma2, 00133 Rome, Italy
[2] Dip. di Fisica, Universita' di Roma "La Sapienza" and INFN, sez. Roma, 00185 Rome, Italy
[3] Laboratori Nazionali del Gran Sasso, I.N.F.N., Assergi, Italy
[4] IHEP, Chinese Academy, P.O. Box 918/3, Beijing 100039, China
[5] Laboratory of Nuclear and High Energy Physics, University of Zaragoza, 50009 Zaragoza, Spain
[6] Dip. di Fisica, Universita' di Roma "Tor Vergata", 00133 Rome, Italy
[7] INAF, Osservatorio Astronomico di Roma, 00040 Monte Porzio Catone, Italy

Received: 13 March 2006 /
Published online: 19 May 2006 –

Abstract. Galaxy hierarchical formation theories, numerical simulations, the discovery of the Sagittarius Dwarf Elliptical Galaxy (SagDEG) in 1994 and more recent investigations suggest that the dark halo of the Milky Way can have a rich phenomenology containing non-thermalized substructures. In the present preliminary study, we investigate the case of the SagDEG (the best known satellite galaxy in the Milky Way crossing the solar neighborhood) analyzing the consequences of its dark matter stream contribution to the galactic halo on the basis of the DAMA/NaI annual modulation data. The present analysis is restricted to some WIMP candidates and to some of the astrophysical, nuclear and particle physics scenarios. Other candidates such as e.g. the light bosonic ones we discussed elsewhere, and other non-thermalized substructures are not yet addressed here.

PACS. 95.35.+d

1 Introduction

The DAMA/NaI set-up [1–4] has exploited the model independent annual modulation signature over seven annual cycles [1–12], achieving 6.3σ C.L. model independent evidence for the presence of a dark matter (DM) particle component in the galactic halo. Some of the many possible corollary quests for the candidate particle have been carried out both on the WIMP class of DM candidate particles with various features and increasing exposures and on keV-range pseudoscalar and scalar DM candidate particles (to which experimental activities, applying whatever rejection technique of the electromagnetic component of the counting rate, are blind). Various possibilities for the candidate and the interactions have also been discussed in the literature by e.g. [13–19].

Many of the uncertainties and assumptions affecting whatever kind of model dependent result in the field (such as e.g. corollary quests for candidate, exclusion plots, and – in the case of indirect investigation experiments – the determination of evidence itself, of the parameters or of the limits, etc.) have been discussed in some detail, e.g. in [3].

Here we will make a preliminary investigation on the effect of DM stream contributions in the galactic halo restricting the presentation to some solutions for the WIMP class already discussed e.g. in [3, 4] and – as regards the stream contribution – to the SagDEG case, which has been already addressed in a different way in the literature, e.g. in [20, 21]. Other interesting cases and candidates will be further addressed in this light in future work.

As known, DAMA/NaI exploited the effect of the earth revolution around the sun on the DM particles' interactions in the target-material of suitable underground detectors. As a consequence of its annual revolution, the earth should be crossed by a variable flux of DM particles along the year. In particular, the expected differential rate as a function of the recoil energy, $\mathrm{d}R/\mathrm{d}E_{\mathrm{R}}$ (see [3] for a detailed discussion), depends on time owing to the DM particle velocity distribution in the laboratory frame, $f(\mathbf{v}|\mathbf{v}_{\oplus}(t))$; here $\mathbf{v}_{\oplus}(t)$ is the earth's velocity in the galactic frame as a function of time.

This method offers an efficient model independent signature, able to test a large interval of cross sections and of halo densities; it is named annual modulation signature and was originally suggested in the middle of the eighties by [22].

[a] e-mail: rita.bernabei@roma2.infn.it
[b] also University of Jing Gangshan, Jiangxi, China

In particular the expected counting rate averaged in a given energy interval can be expressed by the first order Taylor approximation: $S(t) \simeq S_0 + S_{\rm m}\cos\omega(t-t_0)$ with the contribution from the highest order terms less than 0.1%. S_0 is the unmodulated term, $S_{\rm m}$ is the modulation amplitude, $\omega = 2\pi/T$ with $T = 1$ year and t_0 the time when the expected counting rate is maximum. This depends on the adopted halo model and on possible non-thermalized contributions. In particular, for halo models with a velocity distribution isotropic in the galactic frame t_0 is roughly June 2nd, when the earth velocity in the galactic frame is maximal. In the present paper we use the following prescription for the velocity distribution in the laboratory frame once one fixed the halo model: $\rho_{\rm tot} \times f(\mathbf{v}|\mathbf{v}_\oplus(t)) = \rho_{\rm halo} \times f_{\rm halo}(\mathbf{v}|\mathbf{v}_\oplus(t)) + \rho_{\rm stream} \times f_{\rm stream}(\mathbf{v}|\mathbf{v}_\oplus(t))$, where the two contributions of the DM particles in the dark halo and the DM particles in the stream have been made explicit. Here $\rho_{\rm tot}$, $\rho_{\rm halo}$ and $\rho_{\rm stream}$ are the DM particle densities and $f_{\rm halo}$ and $f_{\rm stream}$ are the velocity distributions of the two components normalized to one.

2 SagDEG phenomenology

Since the discovery of the SagDEG in 1994 [23], it has been argued that the dark halo of the Milky Way can have a rich phenomenology containing non-thermalized substructures. This hypothesis is also supported by galaxy hierarchical formation theories [24] and by some numerical simulations [25]. Additional interest is offered by the observation of other satellites of the Milky Way, such as the Canis Major in 2003 [26], and satellites of other near galaxies, like the stream ($v \sim 300$ km/s) discovered in our nearest neighboring "twin" galaxy M31 [27]. In 1998 it was found that the SagDEG orbits the Milky Way in about 10^9 years, having passed through the dense central region of our galaxy at least about 10 times during its life. This has been interpreted as an indication of the presence of DM that with its gravity has prevented the disruption of the SagDEG [28].

Suitable DM direct detection experiments can provide interesting information about the local halo structure, investigating the presence of non-thermalized dark matter fluxes, as in the case of the tidal stream of a dwarf satellite galaxy passing through the solar neighborhood. SagDEG is the best known satellite galaxy of the Milky Way crossing the solar neighborhood; here the consequences of its dark matter stream contribution to the galactic halo are analyzed on the basis of the DAMA/NaI annual modulation data [1–12]. In fact, e.g. – as reported in [4] – the presence of DM streams in the galaxy would induce a (slight) variation of the phase value of the modulated component of the signal and its variation with energy. Consequently, also the $\frac{S_{\rm m}}{S_0}$ ratio undergoes a change depending on the energy window and on the stream properties[1].

[1] In particular, the $\frac{S_{\rm m}}{S_0}$ ratio would increase or decrease to be compared to the absence of stream in the galactic halo depending on the local direction of the stream in the halo.

The SDSS and the 2MASS surveys [29, 30] have traced the tidal stream of the SagDEG; two streams of stars are being tidally pulled away from its main body and extend outward from it. The leading tail can shower matter down through the solar neighborhood, and considerations based on the (very uncertain) M/L ratio suggest the allowed density in the SagDEG tail, $\rho_{\rm sgr}$, to be of the order of (0.001–0.07) GeV cm^{-3} corresponding to about (0.3–23)% of the halo local density [20].

Fundamental information, in order to investigate the effects correlated with the presence of such tidal streams, is the value of the mean velocity of the stream, its direction and its velocity dispersion. Despite the fact that SagDEG is the best known satellite galaxy of the Milky Way crossing the solar neighborhood, these quantities are not yet well defined and a large number of related investigations can be found in literature. In particular, in this paper we have taken into account both the values of [20] (derived from the analysis of eight clump stars – from Chiba and Yoshii catalogue [31] – attributed to the SagDEG tail) and the values of [32] (based on a SagDEG simulation model).

In the following, we will use a right-handed reference frame with the x axis towards the galactic center, the y axis towards the direction of Galaxy rotation and the z axis towards the galactic north pole.

To account for the determination of [20], the SagDEG stream has been modeled as a DM flux with mean velocity in galactic coordinates given by

$$\mathbf{V}_{8*} = (V_x, V_y, V_z) = (-65 \pm 22, 135 \pm 12, -249 \pm 6)\,\text{km/s}. \quad (1)$$

Here a 1σ error has been reported for each velocity component. In addition, to account for the determination of [32] we have also considered the following cases:

$$\mathbf{V}_{\rm sph} = (V_x, V_y, V_z) = (-86 \pm 14, 69 \pm 3, -384 \pm 1)\,\text{km/s}, \quad (2)$$

and

$$\mathbf{V}_{\rm obl} = (V_x, V_y, V_z) = (-57 \pm 8, 79 \pm 3, -395 \pm 1)\,\text{km/s}, \quad (3)$$

for the spherical and the oblate halo models of [32], respectively. These two last stream mean velocities have been derived by considering for each halo model the $\simeq 100$ configurations nearest to the sun within a distance $\lesssim 2.5$ kpc (see Fig. 1). It is worth to note that the prolate model of [32] has not been considered in the following, since no configuration is present in the solar neighborhood. A graphical representation of the three stream mean velocity sets, considered in the present paper for the SagDEG tidal stream, is shown in Fig. 2.

As regards the velocity dispersion to be associated with each one of the three considered stream parametrizations given above, we derive for our reference frame, respectively:

$$(\sigma_x, \sigma_y, \sigma_z)_{8*} = (62, 33, 17)\,\text{km/s}, \quad (4)$$

$$(\sigma_x, \sigma_y, \sigma_z)_{\rm sph} = (60, 19, 8)\,\text{km/s} \quad (5)$$

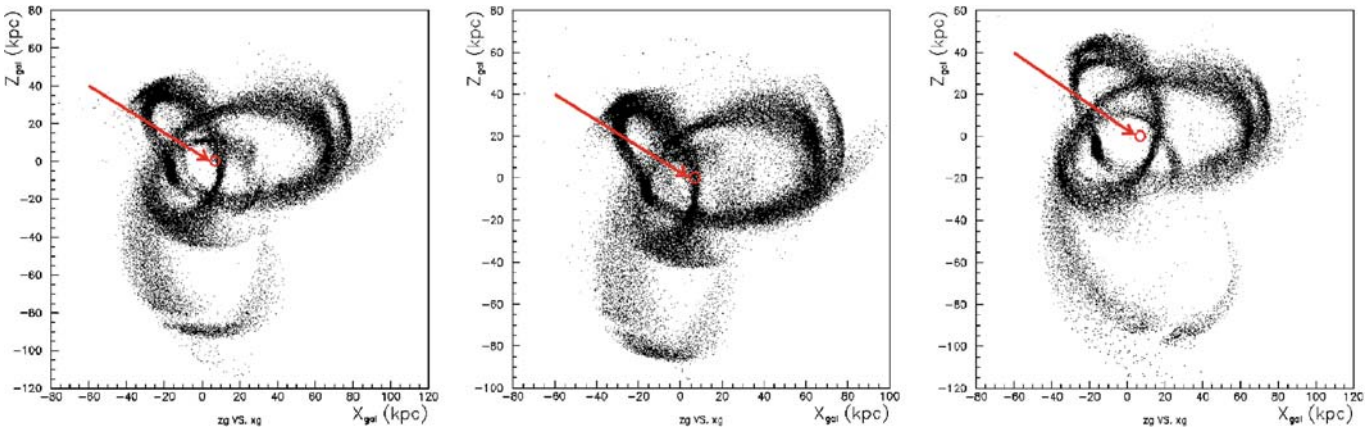

Fig. 1. SagDEG simulation models for spherical (*left*), oblate (*center*) and prolate (*right*) halo potentials; data taken from [32]. In each panel the circle pointed by the arrow selects the earth position and the configurations considered in this paper for the evaluation of the used mean velocity values: $\mathbf{V}_{\rm sph}$ and $\mathbf{V}_{\rm obl}$. We note that no configuration is present in the solar neighborhood for the prolate model

and

$$(\sigma_x, \sigma_y, \sigma_z)_{\rm obl} = (59, 23, 9)\,{\rm km/s}. \quad (6)$$

The $(\sigma_x, \sigma_y, \sigma_z)_{8*}$ is taken from [20], while $(\sigma_x, \sigma_y, \sigma_z)_{\rm sph}$ and $(\sigma_x, \sigma_y, \sigma_z)_{\rm obl}$ have been calculated for each model as r.m.s. values of the about 100 configurations in the solar neighborhood. As it can be observed, for the three considered SagDEG stream models, the velocity dispersions are quite different and significantly non-isotropic. Notwithstanding this, in the following for simplicity the velocity distribution of the SagDEG stream in the solar neighborhood has been approximated by an isotropic Maxwellian distribution in the locally comoving frame of SagDEG. The investigation of the effect of non-isotropic distributions is not considered in the present paper and can be addressed in future.

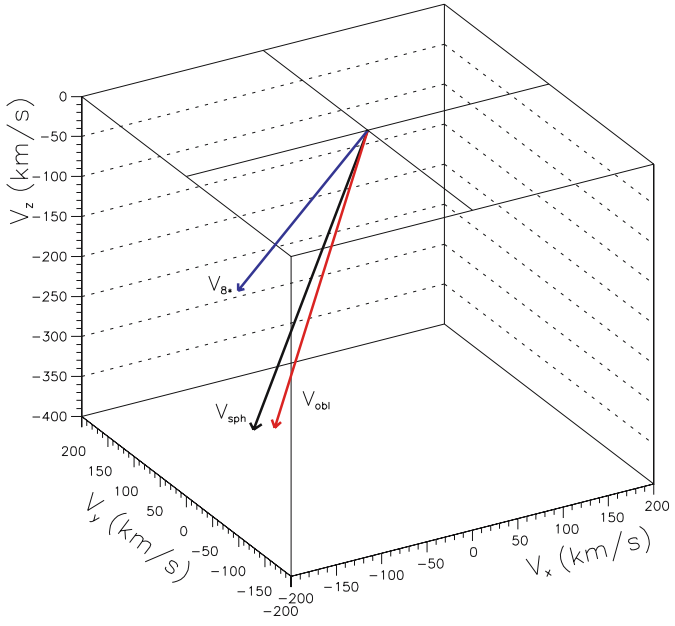

Fig. 2. Graphical representation of the three stream mean velocity sets studied in the present paper for the SagDEG tidal stream

2.1 A full example of the SagDEG effect on the annual modulation signature for a given scenario

In this subsection we show for template purpose a complete example of the effect induced by the presence of a DM stream in the solar neighborhood considering a particular scenario.

As is known, the earth velocity in galactic coordinates can be expressed as follows:

$$\mathbf{v}_\oplus(t) = \mathbf{v}_{\rm LSR} + \mathbf{v}_\odot + V_{\rm earth}(\hat{e}_1 \sin\lambda(t) - \hat{e}_2 \cos\lambda(t))\,, \quad (7)$$

where $\mathbf{v}_{\rm LSR} = (0, 220 \pm 50, 0)$ km/s (the quoted uncertainty is at 90% C.L.) is the velocity of the local standard of rest; $\mathbf{v}_\odot = (10.00, 5.25, 7.17)$ km/s is the sun's peculiar velocity here taken from [33] and $V_{\rm earth}$ is the mean orbital velocity of the earth ($\simeq 29.8$ km/s). The $\hat{e}_1$ and $\hat{e}_2$ unit vectors and the $\lambda(t)$ function are [21]

$$\hat{e}_1 = (-0.0670, 0.4927, -0.8676)\,,$$
$$\hat{e}_2 = (-0.9931, -0.1170, 0.01032)\,,$$
$$\lambda(t) = \omega(t - 0.218)\,.$$

Here $\omega = 2\pi/T$ with $T = 1$ yr, t is the time in years starting from January 1st and 0.218 yr is the spring equinox (March 21).

The velocity distribution of the SagDEG DM particles in the laboratory frame can be written as[2]

$$f_{\rm sgr}(\mathbf{v}) = \frac{1}{\pi^{\frac{3}{2}} v_{0,{\rm sgr}}^3} {\rm e}^{-\frac{(\mathbf{v}-\mathbf{v}_{{\rm sgr},\oplus})^2}{v_{0,{\rm sgr}}^2}}\,, \quad (8)$$

[2] We note that in the following, the quantities related to SagDEG are marked as sgr.

where the mean velocity of the SagDEG DM particles in the laboratory frame is $\mathbf{v}_{\rm sgr,\oplus}(t) = \mathbf{v}_{\rm sgr} - \mathbf{v}_{\oplus}(t)$; $\mathbf{v}_{\rm sgr}$ will be in turn either $\mathbf{V}_{8*}$ or $\mathbf{V}_{\rm sph}$ or $\mathbf{V}_{\rm obl}$. Finally, for each $\mathbf{v}_{\rm sgr}$, the $v_{0,\rm sgr} = \sqrt{\frac{2}{3}}\sigma_{\rm sgr}$ parameter is assumed in the following to be either 20 or 40 or 60 km/s.

The $|\mathbf{v}_{\rm sgr,\oplus}(t)|$ reaches its maximum value at time $t_{0,\rm sgr}$ defined by

$$\cos\left[\lambda(t_{0,\rm sgr})\right] = \frac{a_2}{\sqrt{a_1^2+a_2^2}}\,, \qquad \sin\left[\lambda(t_{0,\rm sgr})\right] = -\frac{a_1}{\sqrt{a_1^2+a_2^2}}\,, \tag{9}$$

with $a_i = \hat{e}_i \cdot (\mathbf{v}_{\rm sgr} - \mathbf{v}_{\rm LSR} - \mathbf{v}_{\odot})$. Therefore, the mean velocity of the SagDEG DM particles in the laboratory frame would be maximum around January 10th–14th, depending on the considered SagDEG velocity set. We remind the reader that in absence of a SagDEG contribution (that is, $f_{\rm halo}$ only contributes to the total DM particles velocity distribution), t_0 is expected to be roughly at the 152.5 day of the year ($\sim$ June 2nd). Hence, the net effect of a SagDEG tail contribution to the local halo density is a shift of few days (towards January) in the expected phase of the signal. For the sake of completeness, the $\frac{S_{\rm m}}{S_0}$ ratio is not expected to be enhanced when a SagDEG stream is included, due to the nearly opposite phases between the two extreme cases.

As examples, in Fig. 3 the phases, t_0, of the modulated component of the signal are plotted for some models with the inclusion of the SagDEG stream and for some reference WIMP masses as a function of the detected energy in NaI(Tl) detectors.

In particular, in the given examples, simple assumptions have been adopted:

i) $\mathbf{v}_{\rm sgr} = (-65, 135, -249)$ km/s, that is, $\mathbf{V}_{8*}$ at its central value;
ii) $v_{0,\rm sgr} = 40$ km/s;
iii) $\mathbf{v}_{\rm LSR} = (0, 220, 0)$ km/s, that is, at its central value;
iv) SagDEG tail DM density $\rho_{\rm sgr} = 0.04 \times \rho_{\rm halo}$;
v) For the galactic halo model: NFW ($\alpha = 1, \beta = 3, \gamma = 1$, $a = 20$ kpc) (A5 of [3]);
vi) WIMP DM candidate with dominant spin independent coupling ($\sigma \propto A^2$);
vii) Form factors and quenching factors of ^{23}Na and ^{127}I as in case A of [3]; that is, the most cautious Helm form factor, the mean nominal values for the parameters of the nuclear form factors and for the measured ^{23}Na and ^{127}I quenching factors are assumed.

For the sake of completeness, we recall that the DAMA/NaI results (107 731 kg · day exposure) provide $t_0 = (140 \pm 22)$ day averaged in the (2–6) keV energy window; at the present level of sensitivity – as it can be seen in Fig. 3 and extensively in the following sections – it is consistent both with the presence and with the absence of a SagDEG contribution. As discussed in [4] larger exposures, which will be available in the near future thanks to the presently running DAMA/LIBRA set-up [34], will offer the possibility of more stringent constraints.

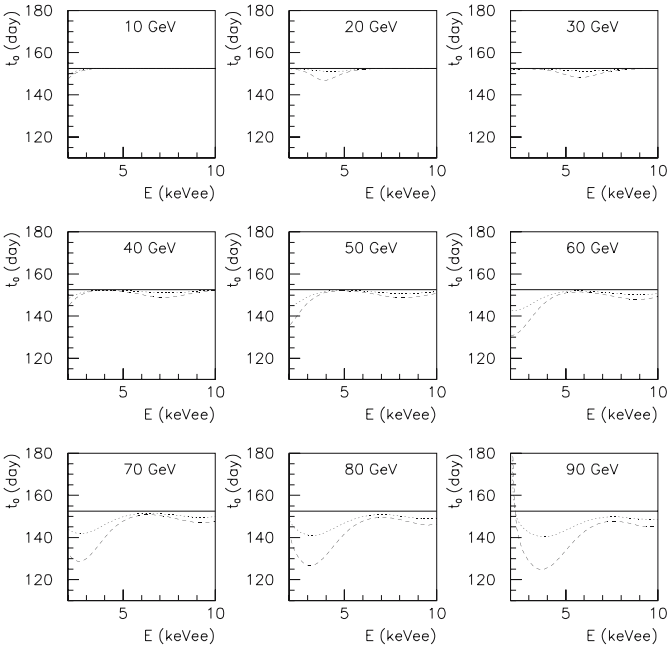

Fig. 3. Examples of the effect of the SagDEG tail, modeled as given in the text, on the expected annual modulation signature in NaI(Tl) detectors. In each panel a plot of the phase (t_0) versus the detected energy (E) is shown for a given WIMP mass and for the given assumptions (see text). *Dotted line*: $\rho_{\rm halo} = 0.74$ GeV cm^{-3} (maximum value allowed for the adopted halo model) [3]; *dashed line*: $\rho_{\rm halo} = 0.33$ GeV cm^{-3} (minimum value allowed for the adopted halo model) [3]; *solid line*: absence of SagDEG contribution, that is $t_0 \sim$ June 2nd. The effect of a possible SagDEG contribution is to slightly shift the phase t_0 towards lower values at low recoil energy

2.2 Investigating the effect of a SagDEG contribution for WIMP cases

In order to further investigate the effect of the presence of a SagDEG stream, we will follow in this section the same approach as exploited in [3, 4], where the simpler case without a SagDEG contribution was considered. In particular we have considered here the WIMP class of candidate particles in the general case of mixed SI (spin independent) and SD (spin dependent) coupling and the two subcases of pure SI and pure SD couplings.

In fact, since the ^{23}Na and ^{127}I are fully sensitive to both SI and SD interactions the most general case is given by a four-dimensional volume ($m_{\rm W}$, $\xi\sigma_{\rm SI}$, $\xi\sigma_{\rm SD}$, θ), where $m_{\rm W}$ is the DM particle mass, ξ is the ratio between the local density for the considered candidate and the local DM density $\rho_{\rm tot}$, $\sigma_{\rm SI}$ is the SI WIMP–nucleon cross section and $\sigma_{\rm SD}$ is the SD WIMP–nucleon cross section according to the definitions and scaling laws considered in [3]; $\tan\theta$ is the ratio between the effective coupling strengths to neutron and proton for the SD couplings (θ can vary between 0 and π). In the calculation the same galactic halo models and associated parameters as in [3] have been considered as well as the uncertainty on the value of the local velocity $v_0 = (220 \pm 50)$ km/s (90% C.L.). For the case of

the SagDEG stream description we have considered the three possibilities for the velocity ($\mathbf{V}_{8*}$, $\mathbf{V}_{\rm sph}$ and $\mathbf{V}_{\rm obl}$ at their central values) and three possible velocity dispersions ($v_{0,\rm sgr} = 20, 40, 60\,$km/s), obtaining nine different cases for each fixed halo model. Moreover, in this section we consider that the SagDEG contribution cannot exceed $\sim$0.1 GeV cm^{-3}, as suggested by the M/L ratio considerations of [20].

The results presented by DAMA/NaI on the corollary searches for the WIMP candidate particles over the seven annual cycles are calculated here and elsewhere (see e.g. [3, 4] and references therein), taking into account the time and energy behaviors of the single-hit experimental data. For this purpose, the likelihood function $L^{i_{\rm m}}_{i_{\rm s},\rho_{\rm sgr}}(m_{\rm W}, \xi\sigma_{\rm SI}, \xi\sigma_{\rm SD}, \theta)$ is constructed for any fixed SagDEG velocity set and velocity dispersion (cumulatively labeled here as $i_{\rm s}$) and for all the considered model frameworks (cumulatively labeled here as $i_{\rm m}$, running on the galactic halo models and on all the other parameters involved in the calculation). In particular, the likelihood function requires the agreement:

i) of the expectations for the modulated part of the signal with the measured modulated behavior for each detector and for each energy bin;
ii) of the expectations for the unmodulated component of the signal with the respect to the measured differential energy distribution;
iii) for WIMP candidate also with the bound on recoils obtained by pulse shape discrimination from the devoted DAMA/NaI-0 data [35].

The latter one (used when WIMP candidates are considered) acts in the likelihood procedure as an experimental upper bound on the unmodulated component of the signal and – as a matter of fact – as an experimental lower bound on the estimate of the background levels by the maximum likelihood procedure. Thus, the C.L. we quote for the allowed regions already account for the compatibility with the measured differential energy spectrum and, – for WIMP candidates – with the measured upper bound on recoils. In particular, in the following, for simplicity, the results of these corollary quests for the candidate particle are presented in terms of allowed regions obtained as a superposition of the configurations corresponding to likelihood function values far more than 4σ from the null hypothesis (absence of modulation) in each of the several ones (but still a limited number) of the possible model frameworks considered here. Obviously, these results are not exhaustive of the many scenarios possible at present level of knowledge (for some other recent ideas see e.g. [36, 37]) and larger sensitivities than those reported in the following would be reached when including the effect of other existing uncertainties on the assumptions and related parameters [3, 4].

For the general case of a WIMP with mixed SI and SD coupling, one obtains a four-dimensional allowed volume[3].

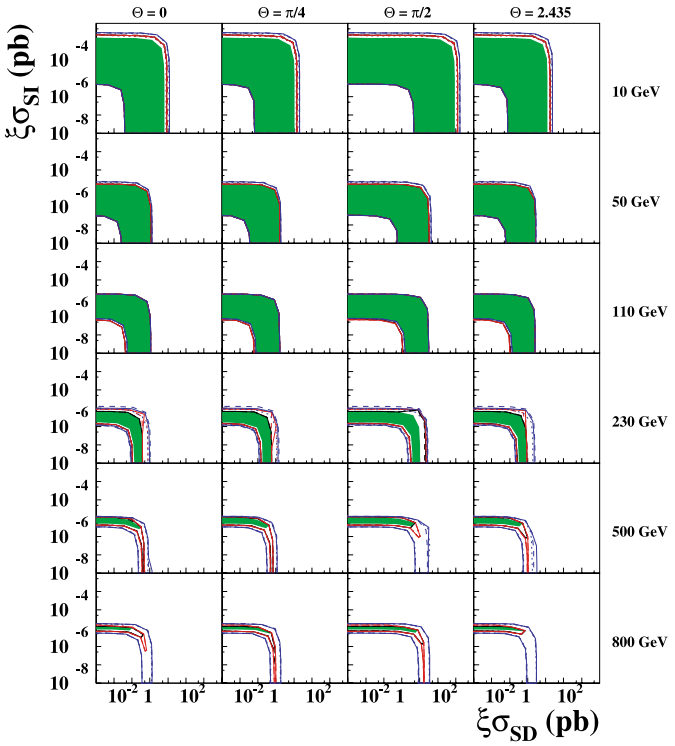

Fig. 4. Examples of slices of the four-dimensional allowed volume in the $(\xi\sigma_{\rm SI}, \xi\sigma_{\rm SD})$ plane for some $m_{\rm W}$ and θ values in the considered scenarios. The shaded regions have been determined for no SagDEG contribution [3], while the areas enclosed by the lines are obtained by introducing in the analysis the SagDEG stream with DM density not larger than 0.1 GeV cm^{-3}. The nine considered possibilities for the SagDEG stream velocity ($\mathbf{V}_{8*}$ (*blue*), $\mathbf{V}_{\rm sph}$ (*black*), $\mathbf{V}_{\rm obl}$ (*red*)) and $v_{0,\rm sgr}$ dispersion (20 km/s (*dashed*), 40 km/s (*solid*) and 60 km/s (*dotted*)) have been reported

Since a full picture of this result is not possible in practice, Fig. 4 shows some slices of the four-dimensional allowed volume in the plane $\xi\sigma_{\rm SI}$ versus $\xi\sigma_{\rm SD}$ for some of the possible $m_{\rm W}$ and θ values. The filled areas show the case without SagDEG contribution and, therefore, have already been reported and discussed in [3, 4] (some different slices are also shown here), while the areas enclosed by lines show the cumulative effect of the possible SagDEG stream contribution in various cases (see the figure caption).

The purely SI subcase[4] is shown in Fig. 5, while in Fig. 6 some slices of the three-dimensional allowed volume ($m_{\rm W}$, $\xi\sigma_{\rm SD}$, θ) for the purely SD case are given. The filled areas

[3] It is worthwhile to note that for example experiments using either nuclei largely insensitive to SD coupling (like e.g. $^{\rm nat}$Ge, $^{\rm nat}$Si, $^{\rm nat}$Ar, $^{\rm nat}$Ca, $^{\rm nat}$W, $^{\rm nat}$O) or nuclei in principle all sensitive to such a coupling but having a different unpaired nucleon (neutron in odd spin nuclei, such as ^{129}Xe, ^{131}Xe, ^{125}Te, ^{73}Ge, ^{29}Si, ^{183}W) with respect to the proton in ^{23}Na and ^{127}I cannot explore most of the four-dimensional allowed volume.

[4] We recall that no direct comparison is possible also among results on purely SI coupled WIMPs achieved by using different nuclei, although apparently all the presentations generally refer to the cross section on the nucleon. For some discussion of generalities and comparisons see e.g. [3, 4, 38].

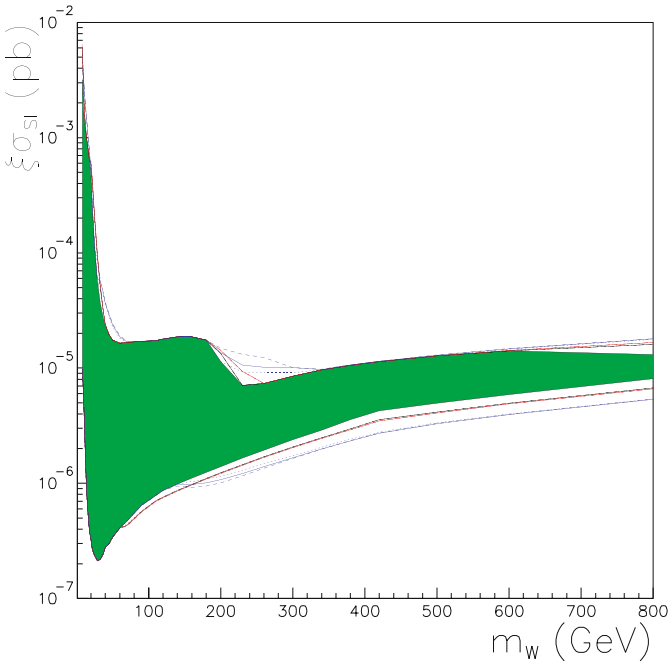

Fig. 5. Region allowed in the $(\xi\sigma_{\rm SI}, m_{\rm W})$ plane in the considered scenarios for pure SI coupling. The filled region has been determined for no SagDEG contribution [3, 4], while the areas enclosed by lines are obtained by introducing in the analysis the SagDEG stream with DM density not larger than 0.1 GeV cm^{-3}. The nine considered possibilities for the SagDEG stream velocity ($\mathbf{V}_{8*}$ (*blue*), $\mathbf{V}_{\rm sph}$ (*black*), $\mathbf{V}_{\rm obl}$ (*red*)) and $v_{0,\rm sgr}$ dispersion (20 km/s (*dashed*), 40 km/s (*solid*) and 60 km/s (*dotted*)) have been reported

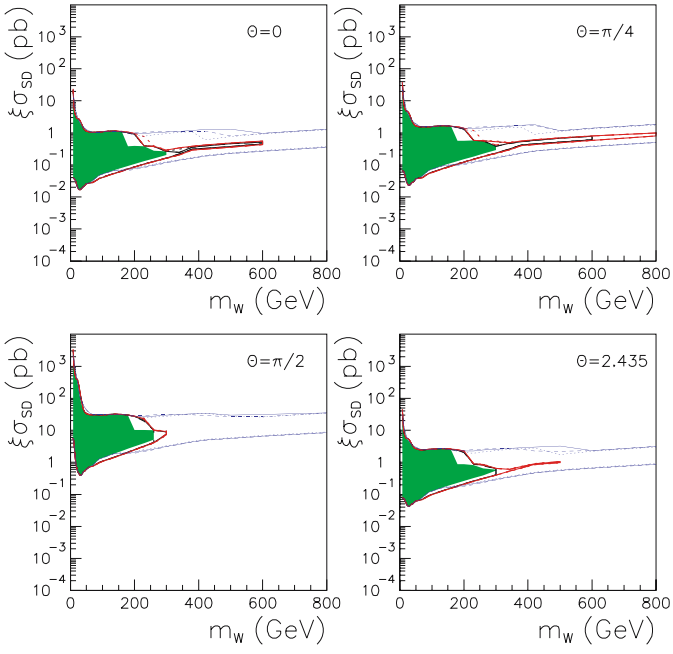

Fig. 6. Examples of slices of the three-dimensional allowed volume in the $(\xi\sigma_{\rm SD}, m_{\rm W})$ plane for some θ values in the considered scenarios and for pure SD coupling. See Fig. 5 for the meaning of the regions

and the areas enclosed by the lines have the same meaning as before.

As it can be observed, the inclusion of the SagDEG stream and of the related uncertainties significantly modifies the allowed volumes/regions; the role appears larger mainly for larger WIMP masses.

It is worth to note that other streams can potentially play more intriguing roles and will be investigated in the near future, such as the Canis Major [26]. Moreover, other kinds of streams as those e.g. arising from caustic halo models [37] can also play a significant role in the corollary investigations for the candidate particle with whatever approach and for comparisons.

This approach to the problem allows us to make some cautious constraints on the SagDEG stream in the galactic halo on the basis of the measured DAMA/NaI annual modulation data. We will discuss some of the implications of the presented results in the next section.

3 Constraining the SagDEG stream by DAMA/NaI

As mentioned, the high exposure of DAMA/NaI can allow one to obtain some preliminary information about the presence of substructure in the halo as the SagDEG stream. For this purpose, the likelihood ratio function has been used as statistical analysis approach in the investigation on the SagDEG parameters with respect to all the others involved in the calculation.

In particular, fixing i) a SagDEG velocity set and a velocity dispersion (index $i_{\rm s}$); ii) the WIMP mass (labeled $m_{\rm W}$) and θ; iii) the galactic halo model and all the other parameters involved in the calculation (index $i_{\rm m}$), the likelihood ratio as a function of $\rho_{\rm sgr}$ can be defined by

$$\lambda^{i_{\rm m},i_{\rm s}}_{m_{\rm W}}(\rho_{\rm sgr}) = \frac{\max_{\sigma_{\rm (SI,SD)}}\left[L^{i_{\rm m},i_{\rm s}}_{m_{\rm W}}(\rho_{\rm sgr}=0)\right]}{\max_{\sigma_{\rm (SI,SD)}}\left[L^{i_{\rm m},i_{\rm s}}_{m_{\rm W}}(\rho_{\rm sgr})\right]}\,, \qquad (10)$$

where $\max_{\sigma_{\rm (SI,SD)}}\left[L^{i_{\rm m},i_{\rm s}}_{m_{\rm W}}(\rho_{\rm sgr})\right]$ is the value of the likelihood function maximized with respect to the particle cross sections.

The functions $Y^{i_{\rm m},i_{\rm s}}_{m_{\rm W}}(\rho_{\rm sgr}) = -2\ln(\lambda^{i_{\rm m},i_{\rm s}}_{m_{\rm W}})$ are asymptotically distributed as chi-square with one degree of freedom. Some examples are given in Fig. 7, where three Y functions are plotted for some halo models and for some particle masses in the particular case of a pure SI candidate and a SagDEG stream with velocity set $\mathbf{V}_{\rm sph}$ and velocity dispersion $v_{0,\rm sgr} = 40$ km/s.

In particular, this figure shows three representative cases: i) a model where the SagDEG contribution worsens the data fit (dotted line); ii) a model where the SagDEG contribution improves the data fit providing a C.L. better than 3σ (solid line); iii) a model where the SagDEG contribution improves the data fit providing a C.L. lower than 3σ (dashed line).

In order to investigate the presence of SagDEG, in all the considered halo models and adopted parameter un-

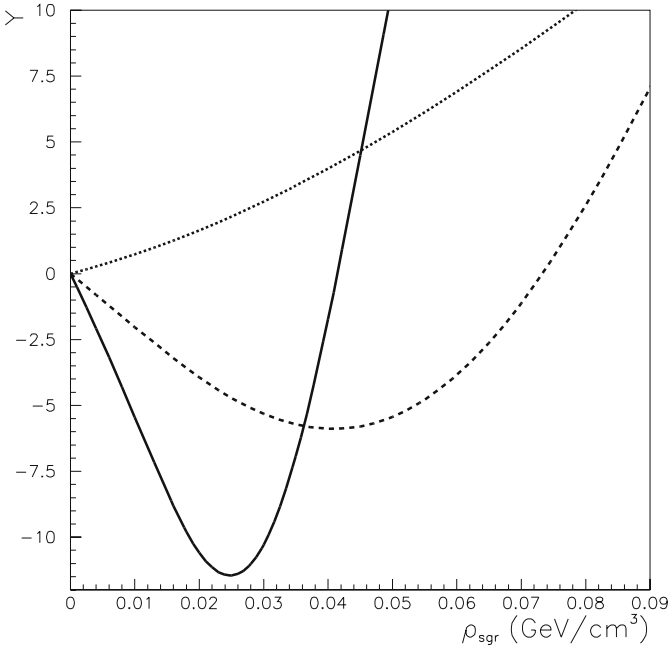

Fig. 7. Effect of the SagDEG contribution in the data fitting for three illustrative models. The example uses: SI candidate, a SagDEG stream with velocity set $\mathbf{V}_{\rm sph}$ and velocity dispersion $v_{0,\rm sgr} = 40$ km/s; all the parameters for form factors and for the quenching factors are fixed at case A of [3] (see also Sect. 2.1 in the text). The considered halo models are i) NFW halo ($\alpha = 1$, $\beta = 3$, $\gamma = 1$, $a = 20$ kpc, A5 of [3]), $v_0 = 220$ km/s, $\rho_{\rm halo} = 0.74$ GeV cm^{-3} and $m_{\rm W} = 10$ GeV (*dotted line*); ii) Evans' logarithmic halo ($R_{\rm c} = 0$ kpc, $q = 1/\sqrt{2}$, C1 of [3]), $v_0 = 170$ km/s, $\rho_{\rm halo} = 0.56$ GeV cm^{-3} and $m_{\rm W} = 22$ GeV (*solid line*); iii) Evans' logarithmic counter-rotating halo ($R_{\rm c} = 5$ kpc, $q = 1/\sqrt{2}$, C2 of [3]), $v_0 = 170$ km/s, $\rho_{\rm halo} = 0.67$ GeV cm^{-3}, $\eta = 0.64$ and $m_{\rm W} = 20$ GeV (*dashed line*)

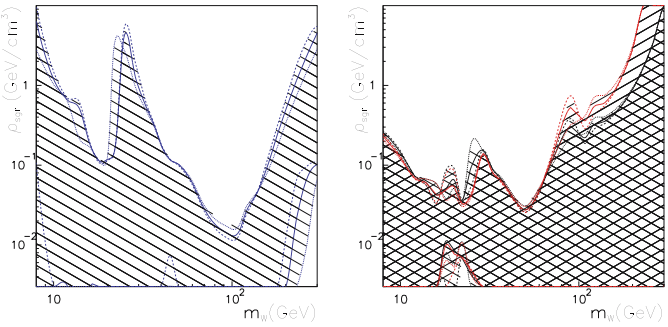

Fig. 8. SagDEG density $\rho_{\rm sgr}$ allowed at 90% C.L. (*hatched area*) for pure SI coupling as a function of $m_{\rm W}$ values. *Left panel*: case of $\mathbf{V}_{8*}$ velocity set. *Right panel*: case of $\mathbf{V}_{\rm sph}$ (*descending hatched*) and $\mathbf{V}_{\rm obl}$ (*ascending hatched*) superimposed. The used stream velocity dispersion, $v_{0,\rm sgr}$, values are 20 km/s (*dashed*), 40 km/s (*solid*) and 60 km/s (*dotted*)

certainties, for simplicity here we alternatively investigate only the purely SI and the purely SD cases, respectively. In the following – for each considered $m_{\rm W}$ and i_s – the 90% C.L. allowed intervals on $\rho_{\rm sgr}$ are constructed requiring that [39]

$$Y^{i_{\rm m},i_{\rm s}}_{m_{\rm W}}(\rho_{\rm sgr}) \leq \min_{(i_{\rm m},\rho_{\rm sgr})}\left(Y^{i_{\rm m},i_{\rm s}}_{m_{\rm W}}(\rho_{\rm sgr})\right) + 2.71\,. \quad (11)$$

In Fig. 8 the SagDEG density $\rho_{\rm sgr}$ allowed at 90% C.L. for pure SI coupling is shown as a function of $m_{\rm W}$. In Fig. 9 the same is shown for a SD coupled candidate in the particular cases of $\theta = 0, \pi/2, \pi/4$ and 2.435 (pure Z_0 coupling).

From Figs. 8 and Fig. 9 upper limits on the SagDEG density can be inferred. In particular, for some WIMP masses and for some halo models, these limits are comparable or improve the limit already given in [20] (of the order of 0.07 GeV cm^{-3}) on the basis of considerations on M/L.

Moreover, Figs. 8 and 9 suggest that intervals not including $\rho_{\rm sgr} = 0$ at 90% C.L. exist for some values of $m_{\rm W}$. This points out a slight preference for the presence of a SagDEG contribution in the data. However, considering the uncertainties on the SagDEG velocity and velocity dispersion (that is e.g. superimposing the allowed regions in Figs. 8 and 9) in most of the considered scenarios the absence of SagDEG is still allowed at 90% C.L.

It is worth to note that in many of the analyzed configurations the inclusion of the SagDEG contribution improves the data fit. For example, for SI candidate in the case of a stream with velocity set $\mathbf{V}_{\rm sph}$ and velocity dispersion $v_{0,\rm sgr} = 40$ km/s, about 67% of the configurations have an improvement of the data fit by the inclusion of the SagDEG; in particular, the improvement of about 18% of them is better than 2σ.

Other interesting information can be inferred by studying the $\rho_{\rm sgr}$ best-fit values achieved for the various considered models. For this purpose, the cumulative percentage distribution of $\rho_{\rm sgr}$ best-fit values providing a C.L. better than 2σ with the respect to the absence of SagDEG is shown in Fig. 10. A pure SI candidate and fixed SagDEG stream with velocity set $\mathbf{V}_{\rm sph}$ and velocity dispersion $v_{0,\rm sgr} = 40$ km/s have been considered here as an example. About 60% of these models gives $\rho_{\rm sgr}$ best-fit values below 0.1 GeV cm^{-3}; in addition, the distribution peaks around $\rho_{\rm sgr} \sim 0.04$ GeV cm^{-3}. These latter values are intriguing, considering the expectations on the stream density at sun position – that is few % of the local dark halo – based on some theoretical studies about the disruption of the satellite galaxies falling in the Milky Way halo [40].

This preliminary analysis offers hints on the possibility to investigate halo features by the annual modulation signature already at the level of sensitivity provided by DAMA/NaI.

4 Conclusion

In this paper a preliminary study on the effect of the presence of dark matter particle streams in the galactic halo has been analyzed on the basis of the annual modulation data collected by DAMA/NaI.

In particular, the case of the Sagittarius Dwarf Elliptical Galaxy (which presently is the better known case)

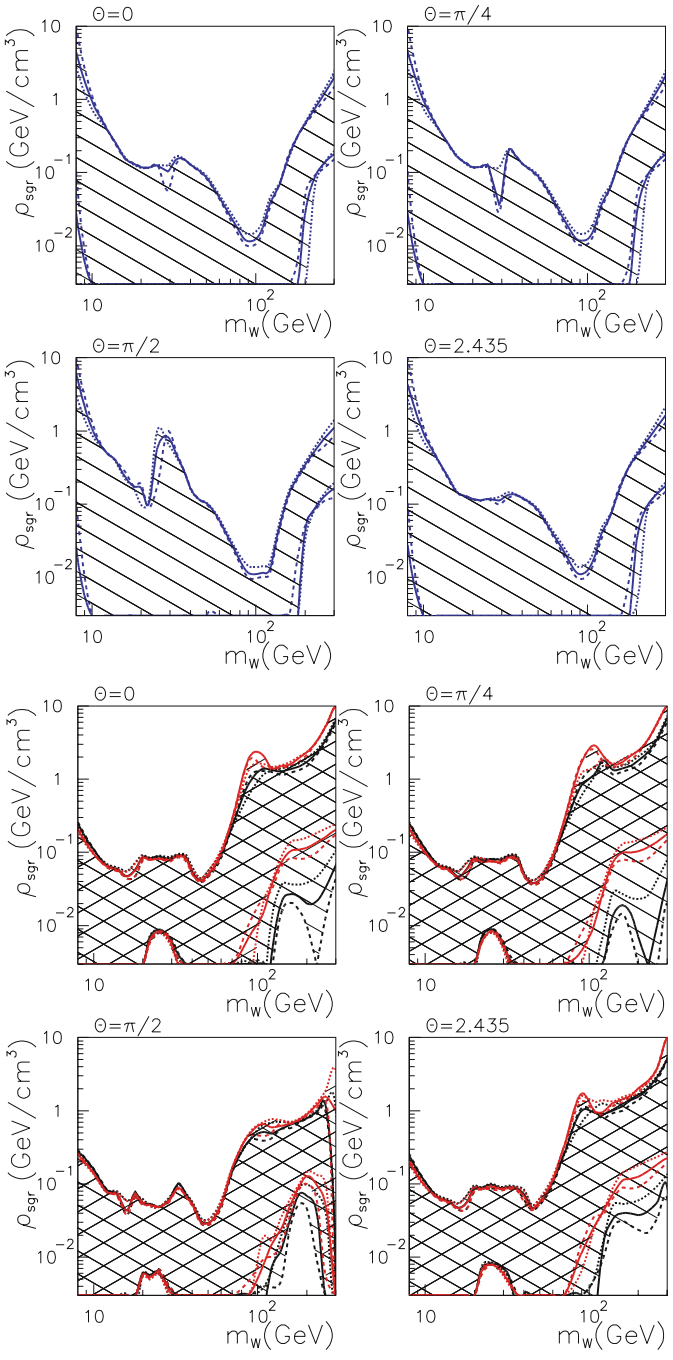

Fig. 9. SagDEG density $\rho_{\rm sgr}$ allowed at 90% C.L. (*hatched area*) for pure SD coupling as a function of $m_{\rm W}$ values for some of the possible θ values. *Upper 4-box*: case of $\mathbf{V}_{8*}$ velocity set. *Lower 4-box*: case of $\mathbf{V}_{\rm sph}$ (*descending hatched*) and $\mathbf{V}_{\rm obl}$ (*ascending hatched*) superimposed. The used stream velocity dispersion, $v_{0,\rm sgr}$ values are 20 km/s (*dashed*), 40 km/s (*solid*) and 60 km/s (*dotted*)

has been discussed here showing its effect on the allowed volumes/regions for some astrophysical, nuclear and particle physics scenarios related to the case of WIMP candidates.

The potentiality of a similar approach to investigate the halo composition has also been pointed out as well as

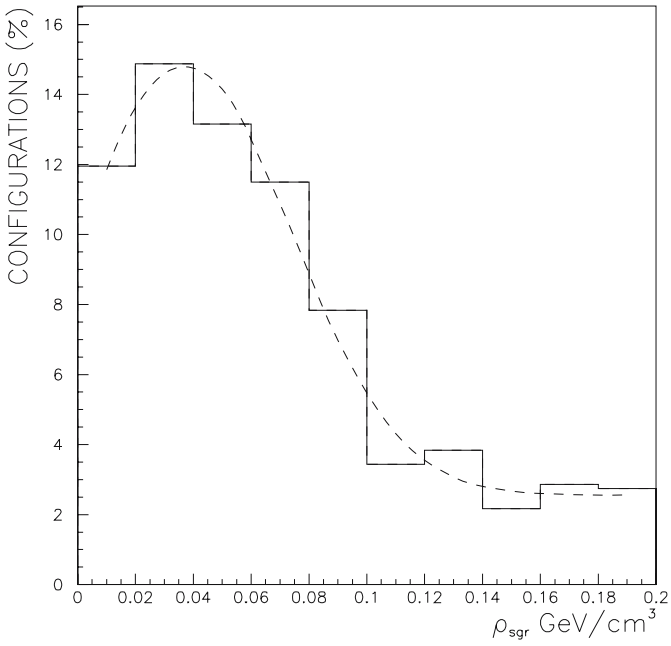

Fig. 10. Example of the cumulative percentage distribution of $\rho_{\rm sgr}$ best-fit values providing a C.L. better than 2σ with the respect to the absence of SagDEG. A pure SI candidate and fixed SagDEG stream with velocity set $\mathbf{V}_{\rm sph}$ and velocity dispersion $v_{0,\rm sgr} = 40$ km/s have been considered. About 60% of these $\rho_{\rm sgr}$ best-fit values are below 0.1 GeV cm^{-3}. See text for implications

the possibility to derive experimental bounds on the possible contribution of the SagDEG to the local dark matter density. For some of the investigated WIMP masses, the order of magnitude of these bounds obtained by local measurements[5] is in agreement with the existing bounds based on non-local M/L ratio observations.

Other candidates and other non-thermalized substructures will be addressed in studies in the near future; in particular, the availability of larger exposures by DAMA/LIBRA will offer the possibility of a more efficient discrimination capability among different possible scenarios.

References

1. R. Bernabei et al., Nuovo Cimento A **112**, 545 (1999)
2. R. Bernabei et al., Eur. Phys. J. C **18**, 283 (2000)
3. R. Bernabei et al., La Rivista del Nuovo Cimento **26**, 1 (2003)
4. R. Bernabei et al., Int. J. Mod. Phys. D **13**, 2127 (2004)
5. R. Bernabei et al., Phys. Lett. B **424**, 195 (1998)
6. R. Bernabei et al., Phys. Lett. B **450**, 448 (1999)
7. P. Belli et al., Phys. Rev. D **61**, 023 512 (2000)
8. R. Bernabei et al., Phys. Lett. B **480**, 23 (2000)
9. R. Bernabei et al., Phys. Lett. B **509**, 197 (2001)

[5] We recall that the local DM density in the solar system is very unconstrained; some limit from precise planet perihelion precession measurements is given for example by $\rho_{\rm Solar\ system} \lesssim 10^6 \rho_{\rm halo}$ [41].

10. R. Bernabei et al., Eur. Phys. J. C **23**, 61 (2002)
11. P. Belli et al., Phys. Rev. D **66**, 043 503 (2002)
12. R. Bernabei et al., Int. J. Mod. Phys. A **21**, 1445 (2006)
13. A. Bottino et al., Phys. Rev. D **67**, 063 519 (2003); A. Bottino et al., Phys. Rev. D **68**, 043 506 (2003)
14. A. Bottino et al., Phys. Rev. D **69**, 037 302 (2004)
15. A. Bottino et al., Phys. Lett. B **402**, 113 (1997); Phys. Lett. B **423**, 109 (1998); Phys. Rev. D **59**, 095 004 (1999); D **59**, 095 003 (1999); Astrop. Phys. **10**, 203 (1999); **13**, 215 (2000); Phys. Rev. D **62**, 056 006 (2000); D **63**, 125 003 (2001); Nucl. Phys. B **608**, 461 (2001)
16. K. Belotsky, D. Fargion, M. Khlopov, R.V. Konoplich, hep-ph/0411093
17. D. Smith, N. Weiner, Phys. Rev. D **64**, 043 502 (2001); D. Smith, N. Weiner, Phys. Rev. D **72**, 063 509 (2005)
18. R. Foot, hep-ph/0308254
19. S. Mitra, Phys. Rev. D **71**, 121 302 (2005)
20. K. Freese et. al., Phys. Rev. D **71**, 043 516 (2005); New Astr. Rev. **49**, 193 (2005); astro-ph/0310334; astro-ph/0309279
21. G. Gelmini, P. Gondolo, Phys. Rev. D **64**, 023 504 (2001)
22. K.A. Drukier et al., Phys. Rev. D **33**, 3495 (1986); K. Freese et al., Phys. Rev. D **37**, 3388 (1988)
23. R.A. Ibata, G. Gilmore, M.J. Irwin, Nature **370**, 194 (1994)
24. J.F. Navarro, C.S. Frenk, S.D.M. White, Ap. J. **462**, 563 (1996)
25. J. Diemand, B. Moore, J. Stadel, Nature **433**, 389 (2005)
26. M. Bellazzini et al., Mon. Not. R. Astronom. Soc. **348**, 12 (2004)
27. S.C. Chapman, New Astr. Rev. **49**, 209 (2005)
28. H. Velazquez, S.D.M. White, Mon. Not. R. Astronom. Soc. L **23**, 275 (1995)
29. H.J. Newberg et al., Ap. J. Lett. **596**, L191 (2003)
30. S.R. Majewski et al., Ap. J. **599**, 1082 (2003)
31. M. Chiba, Y. Yoshii, Astron. J. **115**, 168 (1998)
32. D.R. Law, K.V. Johnston, S.R. Majewski, Ap. J. **619**, 807 (2005); http://www.astro.virginia.edu/∼srm4n/Sgr
33. W. Dehnen, J.J. Binney, Mon. Not. R. Astronom. Soc. **298**, 387 (1998)
34. R. Bernabei et al., in the volume Frontier Objects in Astrophysics and Particle Physics Vol. **90**, 581 (2004)
35. R. Bernabei et al., Phys. Lett. B **389**, 757 (1996)
36. G. Prezeau et al., Phys. Rev. Lett. **91**, 231 301 (2003)
37. F.S. Ling, P. Sikivie, S. Wick, Phys. Rev. D **70**, 123 503 (2004)
38. A. Bottino et al., Phys. Rev. D **72**, 083 521 (2005)
39. S. Eidelman et al., Phys. Lett. B **592**, 1 (2004)
40. D. Stiff, L.M. Widrow, J. Frieman, Phys. Rev. D **64**, 083 516 (2001)
41. I.B. Khriplovich, E.V. Pitjeva, astro-ph/0601422